Non-Markovian spin-resolved counting statistics and an anomalous relation between autocorrelations and cross correlations in a three-terminal quantum dot

JunYan Luo,[1,*] Yiying Yan,[1] Yixiao Huang,[1] Li Yu,[1] Xiao-Ling He,[1] and HuJun Jiao[2]

[1]*Department of Physics, Zhejiang University of Science and Technology, Hangzhou 310023, China*
[2]*Department of Physics, Shanxi University, Taiyuan, Shanxi 030006, China*

We investigate the noise correlations of spin and charge currents through an electron spin resonance (ESR)-pumped quantum dot, which is tunnel coupled to three electrodes maintained at an equivalent chemical potential. A recursive scheme is employed with inclusion of the spin degrees of freedom to account for the spin-resolved counting statistics in the presence of non-Markovian effects due to coupling with a dissipative heat bath. For symmetric spin-up and spin-down tunneling rates, an ESR-induced spin flip mechanism generates a pure spin current without an accompanying net charge current. The stochastic tunneling of spin carriers, however, produces universal shot noises of both charge and spin currents, revealing the effective charge and spin units of quasiparticles in transport. In the case of very asymmetric tunneling rates for opposite spins, an anomalous relationship between noise autocorrelations and cross correlations is revealed, where super-Poissonian autocorrelation is observed in spite of a negative cross correlation. Remarkably, with strong dissipation strength, non-Markovian memory effects give rise to a positive cross correlation of the charge current in the absence of a super-Poissonian autocorrelation. These unique noise features may offer essential methods for exploiting internal spin dynamics and various quasiparticle tunneling processes in mesoscopic transport.

I. INTRODUCTION

Quantum fluctuations in nonequilibrium transport entailed by the granularity of charge are not necessarily detrimental in physical experiments, but may rather unveil intriguing information about the underlying transport processes and dynamics not available from conventional average currents [1]. In particular, recent advances in nanofabrication have made it possible to achieve accurate and highly sensitive on-chip detection of temporal fluctuations in charge or spin currents through quantum systems [2–11]. A complete knowledge of the transport statistics, denoted as full counting statistics (FCS), which characterizes the correlations between quasiparticle transport events to any orders [12–14], can now be extracted experimentally.

The statistics of tunneling processes are normally probed via autocorrelations of the current fluctuations in one terminal of the circuit. For a multiterminal device, an alternative method of measuring the current fluctuations is the cross correlation between two different branches. The principle benefit of employing autocorrelation is that it can be readily accessed in experiments. In particular, for very asymmetric junction capacitances, the autocorrelation is sufficient to characterize the noise spectrum of the entire circuit [1]. However, cross correlation can be utilized to characterize the essential quantum nonlocal properties [15–22]. Furthermore, cross correlation is able to filter out local fluctuations not shared by the two terminals (detectors), leading to a strong enhancement in the signal-to-noise ratio of quantum measurements [23–27]. In reality, both autocorrelation and cross correlation are indispensable to a deep understanding of the transport statistics.

For noninteracting fermions, the Pauli exclusion principle leads to a suppression of noise below the classical Poisson value [28], and correspondingly yields a negative cross correlation in a multiterminal structure [29]. This has been experimentally confirmed in an electronic version of the Hanbury Brown-Twiss experiment [30,31]. In the presence of interactions, however, these restrictions on autocorrelations and cross correlations do not exist, in principle. For instance, it has been demonstrated that super-Poissonian autocorrelations occur in the presence of a dynamical channel (spin) blockade [32–38], or cotunneling events [39–41]. In addition, the sign reversal of cross correlations have been proposed to result from a variety of mechanisms such as crossed Andreev reflection processes [42–44] and the feedback effects of external voltage fluctuations [45]. In particular, positive cross correlations have been experimentally observed in a number of systems such as tunnel junctions [15,46,47], quantum dot (QD) systems [48], and semiconducting nanowires [49]. It is thus appealing to investigate the essential relationships between autocorrelations and cross correlations in the presence of interactions, which can provide information complementary to an understanding of each, and enable a deeper analysis of the underlying physics in quasiparticle transport.

Cross correlations for a three-terminal QD device have been experimentally verified to be proportional to autocorrelations in excess of the Poissonian value, i.e., there are one-to-one correspondences between positive and negative cross correlations and super-Poissonian and sub-Poissonian autocorrelations, respectively [50]. It was later predicted for the case of ferromagnetic electrodes that this relation does not necessary hold, and a super-Poissonian autocorrelation may correspond to a negative cross correlation, depending on the degree of spin polarization in the electrodes [51,52]. This finding, in conjunction with the presently standing observation that positive cross correlations occur only in the presence of super-Poissonian autocorrelations, indicates that
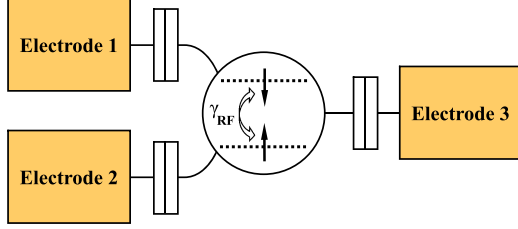
---

*jyluo@zust.edu.cn

FIG. 1. A schematic of an ESR-pumped three-terminal QD system, where the three electrodes are maintained at an equivalent chemical potential located between the spin-up and spin-down single-electron levels, such that only spin-up electrons can tunnel into the QD and spin-down electrons tunnel out.

it is of significant interest and physical importance to establish whether it is possible to obtain positive cross correlation in the absence of super-Poissonian autocorrelation.

In this work, we exam this essential issue in the context of an ESR-pumped spin current through the three-terminal QD, as schematically shown in Fig. 1. Our analysis is based on a generic spin-resolved FCS formalism established with appropriate inclusion of non-Markovian memory effects due to coupling with an external heat bath. We reveal an anomalous relationship between autocorrelations and cross noise correlations. In the limit of very asymmetric spin tunnel couplings, super-Poissonian autocorrelation is observed in spite of a negative cross correlation. In addition, with strong dissipation strength, it is demonstrated unambiguously that positive cross correlation does occur with a sub-Poissoianian autocorrelation in the presence of non-Markovian memory effects.

The remainder of this paper is organized as follows. We begin in Sec. II with a presentation of the ESR-pumped three-terminal QD system. The spin-resolved quantum master equation (QME) is derived in Sec. III, where non-Markovian characteristics are included due to coupling with a dissipative heat bath. To account appropriately for non-Markovian spin transport processes, in Sec. IV we utilize a recursive scheme [53,54] with inclusion of spin degrees of freedom to obtain, in principle, any order of spin-resolved current cumulants. The observation of super-Poissonian autocorrelation with negative cross correlation as well as the occurrence of positive cross correlation despite sub-Poissonian autocorrelation are discussed in Sec. V, where the underlying mechanisms associated with phonon-assisted tunneling processes and non-Markovian memory effects are revealed. Finally, we summarize the work in Sec. VI.

II. MODEL DESCRIPTION

The system under investigation is a Coulomb-blockaded single QD tunnel coupled to three electrodes (Fig. 1), which are maintained at an equivalent chemical potential μ_0. An external rotating magnetic field, $B(t) = B_0(\sin\theta\cos\Omega t, \sin\theta\sin\Omega t, \cos\theta)$, is applied to the QD, where its z component is responsible for the Zeeman splitting of the single-electron level, with the Zeeman energy $\Delta = g_z\mu_B B_0\cos\theta$, g_z the effective electron gyromagnetic factor in the z direction and μ_B the Bohr magneton. The chemical

potential μ_0 is located between the split spin-up and spin-down levels, ensuring that only spin-up electrons can tunnel into the QD and spin-down electrons tunnel out. The frequency Ω of the oscillating magnetic field is tuned very close to Zeeman splitting Δ, leading thus to the well-known electron spin resonance. The spin-up electron in the QD is thereby pumped to the higher level with its spin orientation flipped, which then tunnels out to the electrodes, generating an ESR-pumped spin current. In the strong Coulomb blockade regime, double occupation in the QD is energetically prohibited, such that no additional spin-up electrons can enter the QD prior to the spin-down electron tunneling out. Furthermore, the QD is also coupled to an inevitably dissipative phonon environment, which is not shown explicitly in Fig. 1. The Hamiltonian of the entire system is given as

$$H = H_{\mathrm{QD}} + H_{\mathrm{env}} + H'. \tag{1}$$

Here, H_{QD} represents the Hamiltonian of the single QD in the presence of magnetic fields, H_{env} is the Hamiltonian of the environment, and H' is that of the coupling between the single QD and the environment.

The first term on the right is given as

$$H_{\mathrm{QD}} = \frac{\Delta}{2}Q_z + \gamma_{\mathrm{RF}}(d_\uparrow^\dagger d_\downarrow e^{i\Omega t} + d_\downarrow^\dagger d_\uparrow e^{-i\Omega t}), \tag{2}$$

where the pseudospin operator is defined as $Q_z = d_\downarrow^\dagger d_\downarrow - d_\uparrow^\dagger d_\uparrow$, with $d_\sigma^\dagger$ and d_σ respectively representing the creation and annihilation operators of an electron with spin $\sigma = \uparrow, \downarrow$ in the QD. Spin-up and spin-down states are coupled to each other due to the rotating field, with the ESR Rabi frequency given by $\gamma_{\mathrm{RF}} = g_\perp\mu_B B_0\sin\theta$ and $g_\perp$ the electron gyromagnetic factor in the perpendicular direction. The time dependence of H_{QD} can be eliminated by transforming to a rotating frame via $U(t) = e^{iH_0 t}$ with $H_0 = \frac{1}{2}\Omega Q_z$, leading to the following redefinition:

$$\mathcal{H}_{\mathrm{QD}} = U(t)(H_{\mathrm{QD}} - H_0)U^\dagger(t) = \frac{1}{2}\delta_{\mathrm{ESR}}Q_z + \gamma_{\mathrm{RF}}Q_x, \tag{3}$$

with ESR detuning $\delta_{\mathrm{ESR}} = \Delta - \Omega$ and the pseudospin operator $Q_x = d_\uparrow^\dagger d_\downarrow + d_\downarrow^\dagger d_\uparrow$. The transformation leaves H_{env} and H' unchanged.

H_{env} is comprised of Hamiltonians representative of electron reservoirs H_{res} and the heat bath H_B:

$$H_{\mathrm{env}} = H_{\mathrm{res}} + H_B. \tag{4}$$

Here, $H_{\mathrm{res}} = \sum_{j=1,2,3}\sum_{k\sigma}\epsilon_{jk\sigma}c_{jk\sigma}^\dagger c_{jk\sigma}$ models noninteracting electrons in the electrodes, where $c_{jk\sigma}^\dagger$ ($c_{jk\sigma}$) represents the creation (annihilation) operator for an electron in electrode j ($j = 1,2,3$) with momentum k and spin σ. $H_B = \sum_q\hbar\omega_q a_q^\dagger a_q$ depicts dissipative heat bath, where $a_q^\dagger$ (a_q) denotes the creation (annihilation) operator for a boson in mode q.

The last term in Eq. (1), describing coupling between the single QD and environment, can be written as

$$H' = H_{\mathrm{QD-el}} + H_{\mathrm{QD-ph}}. \tag{5}$$

The first component $H_{\mathrm{QD-el}} = \sum_{j\sigma}(f_{j\sigma}^\dagger d_\sigma + d_\sigma^\dagger f_{j\sigma})$ depicts electron tunneling between QD and electrodes, with $f_{j\sigma} = \sum_k t_{jk\sigma}c_{jk\sigma}$ and $t_{jk\sigma}$ the spin-dependent tunneling amplitude. The corresponding tunneling rate for an electron with

spin σ is characterized by the intrinsic linewidth $\Gamma_{j\sigma}(\omega) = 2\pi \sum_k |t_{jk\sigma}|^2 \delta(\omega - \epsilon_{jk\sigma})$. Hereafter, we assume wide band limit in the electrodes, which leads to energy-independent tunneling rates $\Gamma_{j\sigma}(\omega) = \Gamma_{j\sigma}$. Owing to the position of μ_0 between the two split spin levels, spin-up electrons can tunnel into the QD with rate $\Gamma_{j\uparrow}$ and spin-down electrons tunnel out with rate $\Gamma_{j\downarrow}$. The second component in Eq. (5) models coupling with the phonon bath $H_{QD-ph} = F_B Q_z$, where $F_B = \frac{1}{2}\sum_q \lambda_q(a_q^\dagger + a_q)$, with λ_q the electron-phonon coupling strength. The effect of phonon bath on the QD system is characterized by the phonon interaction spectral density $J(\omega) = \sum_q |\lambda_q|^2 \delta(\omega - \omega_q)$. Here, we consider the case of Ohmic dissipation $J(\omega) = 2\alpha\omega e^{-\omega/\omega_c}$, where the dimensionless parameter α reflects the strength of dissipation and ω_c is the Ohmic high-energy cutoff. In what follows, we set unit of $\hbar = e = 1$ for the Planck constant and electron charge, unless stated otherwise.

III. NON-MARKOVIAN SPIN-RESOLVED QME

The dynamics of the reduced spin system can be described by the QME for a reduced density matrix $\varrho(t)$. However, to describe spin transport characteristics, it is necessary to unravel the density matrix $\varrho(t)$ into components $\varrho(\{N_{j\sigma}\},t)$, where $(\{N_{j\sigma}\}) = (N_{1\uparrow}, N_{1\downarrow}, N_{2\uparrow}, N_{2\downarrow}, N_{3\uparrow}, N_{3\downarrow})$, with $N_{j\sigma}$ the number of spin-σ ($\sigma = \uparrow, \downarrow$) electrons tunneled through junction j ($j = 1,2,3$) during the time span $[0,t]$. This equation, denoted as the spin-resolved QME, can be derived via decomposition of the entire Hilbert space of the electrode reservoirs [55–58] or employing the real-time diagrammatic technique on the Keldysh contour [59–61]:

$$\frac{\partial}{\partial t}\varrho(\{N_{j\sigma}\},t) = \sum_{\{N_{j'\sigma'}\}} \int_0^t dt' \mathcal{W}(\{N_{j\sigma} - N_{j'\sigma'}\}, t - t')$$
$$\times \varrho(\{N_{j'\sigma'}\}, t') + \Upsilon(\{N_{j\sigma}\}, t), \quad (6)$$

where the memory kernel $\mathcal{W}$ describes the influence of the environment (electrodes and heat bath) on the spin dynamics, and the inhomogeneity Υ accounts for the initial correlation between the reduced system and the environment. The spin-resolved density matrix $\varrho(\{N_{j\sigma}\},t)$ is directly associated with the probability distribution for the number of transferred spin $P(\{N_{j\sigma}\},t) = \text{tr}[\varrho(\{N_{j\sigma}\},t)]$, where $\text{tr}[\cdots]$ denotes the trace over the degrees of freedom of the reduced system. The corresponding spin-resolved cumulant generating function (CGF) $\mathcal{F}(\{\chi_{j\sigma}\},t)$ is then given by

$$e^{\mathcal{F}(\{\chi_{j\sigma}\},t)} = \sum_{\{N_{j\sigma}\}} P(\{N_{j\sigma}\},t)e^{i\{N_{j\sigma}\}\cdot\{\chi_{j\sigma}\}}, \quad (7)$$

where $(\{\chi_{j\sigma}\}) = (\chi_{1\uparrow}, \chi_{1\downarrow}, \chi_{2\uparrow}, \chi_{2\downarrow}, \chi_{3\uparrow}, \chi_{3\downarrow})$ are the spin-resolved counting fields associated with $(\{N_{j\sigma}\})$.

By performing a Laplace transform $\tilde{\varrho}(\{\chi_{j\sigma}\},z) = \sum_{\{N_{j\sigma}\}} \int_0^\infty dt' \varrho(\{N_{j\sigma}\},t') e^{i\{N_{j\sigma}\}\cdot\{\chi_{j\sigma}\}-zt'}$, Eq. (6) leads readily to an algebraic equation

$$z\tilde{\varrho} - \varrho(t=0) = \mathcal{W}(\{\chi_{j\sigma}\},z)\tilde{\varrho} + \tilde{\Upsilon}(\{\chi_{j\sigma}\},z). \quad (8)$$

A detailed derivation of this equation is provided in Appendix A. Specifically, let us here consider the spin occupation representation: $|0\rangle$ empty and $|\sigma\rangle$ occupied by a

spin-σ electron. Under this condition, the kernel $\mathcal{W}(\{\chi_{j\sigma}\},z)$ in the Laplace domain is given by (see Appendix A)

$$\mathcal{W}(\{\chi_{j\sigma}\},z) = \begin{pmatrix} -\tilde{\Gamma}_\uparrow^0 & 0 & \tilde{\Gamma}_\downarrow^{\chi_\downarrow} \\ \tilde{\Gamma}_\uparrow^{\chi_\uparrow} & -\gamma_z^+ & \gamma_z^- \\ 0 & \gamma_z^+ & -\gamma_z^- - \tilde{\Gamma}_\downarrow^0 \end{pmatrix}, \quad (9)$$

where $\tilde{\Gamma}_\sigma^{\chi_\sigma} = \sum_{j=1,2,3} \Gamma_{j\sigma} e^{i\chi_{j\sigma}}$ is the counting-field-dressed tunneling width for a spin-σ electron, and $\gamma_z^\pm$ are the bath-assisted hopping rates

$$\gamma_z^\pm = \gamma_{RF}^2 \{\tilde{C}^{(\pm)}(z_+) + \tilde{C}^{(\mp)}(z_-)\}, \quad (10)$$

with $z_\pm = z + \frac{\tilde{\Gamma}_\downarrow^0}{2} \pm i\delta_{ESR}$. The involving $\tilde{C}^{(\pm)}(z)$ are the Laplace transform of the bath correlation functions:

$$\tilde{C}^{(\pm)}(z) = \int_0^\infty dt\, e^{-zt} C^{(\pm)}(t), \quad (11)$$

with

$$C^{(\pm)}(t) = e^{-Q(\mp t)},$$
$$Q(t) = \int_0^\infty d\omega \frac{J(\omega)}{\omega^2}$$
$$\times \left\{ [1 - \cos(\omega t)] \coth\left(\frac{\beta\omega}{2}\right) + i\sin(\omega t) \right\}. \quad (12)$$

The details for the derivation of the bath correlations are given in Appendix B.

It is worthwhile mentioning the validity of our approach. First, for the treatment of coupling to the electronic reservoirs, we employed the standard Born-Markov perturbation. In the context of present ESR-based QD system it requires that the Zeeman splitting Δ and the temperature $k_B T$ are much larger than the tunnel-coupling strength, i.e., $\Delta, k_B T \gg \Gamma_{j\sigma}$. Second, for the coupling to the phonon bath, we performed a polaron transform (see Appendix B), which therefore implies that our approach is applicable to strong heat bath coupling. The resultant equation (6) exhibits clearly non-Markovian characteristics. The conventional Markovian QME approach for the FCS therefore must be extended, such that the non-Markovian effects are appropriately described, as is presented in the following section.

IV. GENERAL FORMALISM FOR NON-MARKOVIAN SPIN-RESOLVED FCS

The spin-resolved CGF given above as $\mathcal{F}(\{\chi_{j\sigma}\},t)$ is the essential component required for evaluating spin-resolved cumulants. For that purpose, we solve Eq. (8) formally as

$$\tilde{\varrho}(\{\chi_{j\sigma}\},z) = \mathcal{G}(\{\chi_{j\sigma}\},z)[\varrho(\{\chi_{j\sigma}\},t=0) + \tilde{\Upsilon}], \quad (13)$$

where

$$\mathcal{G}(\{\chi_{j\sigma}\},z) = [z - \mathcal{W}(\{\chi_{j\sigma}\},z)]^{-1} \quad (14)$$

is the resolvent of the kernel. By returning to the time domain via an inverse Laplace transformation, one readily obtains the

CGF as

$$e^{\mathcal{F}} = \frac{1}{2\pi i} \int_{a-i\infty}^{a+i\infty} dz \, \mathrm{tr}\{\mathcal{G}(\{\boldsymbol{\chi}_{j\sigma}\}, z)[\varrho(\{\boldsymbol{\chi}_{j\sigma}\}, t = 0) + \tilde{\Upsilon}]\}, \tag{15}$$

where a is a real number chosen in such a way that all the singularities of the integrand are located on the left of the vertical integration line. Equation (15) is a powerful result, containing the full statistical information regarding the spin transfer process. For instance, the first zero-frequency cumulants correspond to spin-dependent currents

$$\langle\!\langle I_{j\sigma} \rangle\!\rangle = \frac{d}{dt} \frac{\partial}{\partial(i\chi_{j\sigma})} \mathcal{F}(\{\boldsymbol{\chi}_{j\sigma}\}, t)|_{\{\boldsymbol{\chi}_{j\sigma}\} \to \{\mathbf{0}\}}. \tag{16}$$

The net charge and spin currents through terminal $j \in \{1,2,3\}$ are then given respectively by

$$\langle\!\langle I_j^c \rangle\!\rangle = \langle\!\langle I_{j\uparrow} \rangle\!\rangle + \langle\!\langle I_{j\downarrow} \rangle\!\rangle, \tag{17a}$$

$$\langle\!\langle I_j^s \rangle\!\rangle = \langle\!\langle I_{j\uparrow} \rangle\!\rangle - \langle\!\langle I_{j\downarrow} \rangle\!\rangle. \tag{17b}$$

The second cumulants are related to the spin-resolved shot noise, and are given as

$$\langle\!\langle I_{j\sigma} I_{j'\sigma'} \rangle\!\rangle = \frac{d}{dt} \frac{\partial^2 \mathcal{F}(\{\boldsymbol{\chi}_{j\sigma}\}, t)}{\partial(i\chi_{j\sigma})\partial(i\chi_{j'\sigma'})}|_{\{\boldsymbol{\chi}_{j\sigma}\} \to \{\mathbf{0}\}}, \tag{18}$$

with $j, j' \in \{1,2,3\}$. According to Eq. (17), one readily finds the autocorrelation ($j = j'$) and cross correlation ($j \neq j'$) of the total charge and spin currents

$$\langle\!\langle I_j^c I_{j'}^c \rangle\!\rangle = \langle\!\langle I_{j\uparrow} I_{j'\uparrow} \rangle\!\rangle + \langle\!\langle I_{j\downarrow} I_{j'\downarrow} \rangle\!\rangle + \langle\!\langle I_{j\uparrow} I_{j'\downarrow} \rangle\!\rangle + \langle\!\langle I_{j\downarrow} I_{j'\uparrow} \rangle\!\rangle, \tag{19a}$$

$$\langle\!\langle I_j^s I_{j'}^s \rangle\!\rangle = \langle\!\langle I_{j\uparrow} I_{j'\uparrow} \rangle\!\rangle + \langle\!\langle I_{j\downarrow} I_{j'\downarrow} \rangle\!\rangle - \langle\!\langle I_{j\uparrow} I_{j'\downarrow} \rangle\!\rangle - \langle\!\langle I_{j\downarrow} I_{j'\uparrow} \rangle\!\rangle. \tag{19b}$$

In principle, higher-order cumulants can be obtained in a similar manner.

The zero-frequency cumulants are determined by the long-time behavior of $\mathcal{F}$ [53,54]

$$\mathcal{F}(\{\boldsymbol{\chi}_{j\sigma}\}, t) \to z_0(\{\boldsymbol{\chi}_{j\sigma}\}) t, \tag{20}$$

in which $z_0(\{\boldsymbol{\chi}_\sigma\})$ is a unique pole of the resolvent $\mathcal{G}(\{\boldsymbol{\chi}_{j\sigma}\}, z)$ that satisfies $z_0(\{\mathbf{0}\}) = 0$ and solves

$$z_0(\{\boldsymbol{\chi}_{j\sigma}\}) - \lambda_0(\{\boldsymbol{\chi}_{j\sigma}\}, z_0) = 0. \tag{21}$$

Here, $\lambda_0(\{\boldsymbol{\chi}_{j\sigma}\}, z_0)$ is the single isolated eigenvalue of $\mathcal{W}(\{\boldsymbol{\chi}_{j\sigma}\}, z)$ that evolves adiabatically from $\lambda_0(\{\mathbf{0}\}, z_0) = 0$.

Equations (20) and (21) enable us to calculate the zero-frequency spin-dependent cumulants readily. For instance, the first spin-resolved cumulants are given by

$$\langle\!\langle I_{j\sigma} \rangle\!\rangle = \frac{\partial}{\partial(i\chi_{j\sigma})} \lambda_0|_{\{\boldsymbol{\chi}_{j\sigma}\} \to \{\mathbf{0}\}, z_0 \to 0}. \tag{22}$$

The second cumulants simply read

$$\langle\!\langle I_{j\sigma} I_{j'\sigma'} \rangle\!\rangle = \left\{ \frac{\partial^2}{\partial(i\chi_{j\sigma})\partial(i\chi_{j'\sigma'})} + \langle\!\langle I_{j\sigma} \rangle\!\rangle \frac{\partial^2}{\partial(i\chi_{j'\sigma'})\partial z} \right.$$
$$\left. + \langle\!\langle I_{j'\sigma'} \rangle\!\rangle \frac{\partial^2}{\partial(i\chi_{j\sigma})\partial z} \right\} \lambda_0|_{\{\boldsymbol{\chi}_{j\sigma}\} \to \{\mathbf{0}\}, z_0 \to 0}. \tag{23}$$

While we here present only the first two cumulants, higher-order cumulants can be obtained in a similar fashion.

The dominant eigenvalue $\lambda_0(\{\boldsymbol{\chi}_{j\sigma}\}, z_0)$ can be evaluated in a recursive manner by using the Brillouin-Wigner perturbation theory. The stationary state of the reduced system $|0\rangle\!\rangle = \lim_{t\to\infty} \varrho(t)$ can be obtained as the normalized solution to $\mathcal{W}_0|0\rangle\!\rangle = 0$, with $\mathcal{W}_0 = \mathcal{W}(\{\boldsymbol{\chi}_{j\sigma}\} = \{\mathbf{0}\}, z = 0)$. Analogously, $\langle\!\langle \tilde{0}|$ is the normalized solution to $\langle\!\langle \tilde{0}|\mathcal{W}_0 = 0$, satisfying the normalization condition $\langle\!\langle \tilde{0}|0\rangle\!\rangle = 1$. By introducing the perturbation of the kernel $\overline{\mathcal{W}} = \mathcal{W}(\{\boldsymbol{\chi}_{j\sigma}\}, z) - \mathcal{W}_0$ and its pseudoinverse operator $\mathcal{R} = \mathcal{Q}_0[\lambda_0(\{\boldsymbol{\chi}_{j\sigma}\}, z) - \mathcal{W}_0]^{-1}\mathcal{Q}_0$, where $\mathcal{Q}_0 \equiv 1 - |0\rangle\!\rangle\langle\!\langle \tilde{0}|$, one arrives at a formal expression of the dominant eigenvalue

$$\lambda_0(\{\boldsymbol{\chi}_{j\sigma}\}, z) = \langle\!\langle \tilde{0}|\overline{\mathcal{W}}(1 - \mathcal{R}\overline{\mathcal{W}})^{-1}|0\rangle\!\rangle, \tag{24}$$

which serves as a starting point for the efficient calculation of the spin-resolved cumulants in a recursive manner. The first cumulants, given by Eq. (22), are readily obtained via the first time derivative of $\overline{\mathcal{W}}$ with respect to the counting field:

$$\langle\!\langle I_{j\sigma} \rangle\!\rangle = \left\langle\!\!\left\langle \tilde{0} \left| \frac{\partial \overline{\mathcal{W}}}{\partial(i\chi_{j\sigma})} \right| 0 \right\rangle\!\!\right\rangle_{\{\boldsymbol{\chi}_{j\sigma}\} \to \{\mathbf{0}\}, z \to 0}, \tag{25}$$

which have no z dependence, and, thus are not sensitive to non-Markovian effects. The second spin-resolved cumulants given by Eq. (23), however, clearly show the existence of the non-Markovian influence:

$$\langle\!\langle I_{j\sigma} I_{j'\sigma'} \rangle\!\rangle = \left\langle\!\!\left\langle \tilde{0} \left| \left\{ \frac{\partial^2 \overline{\mathcal{W}}}{\partial(i\chi_{j\sigma})\partial(i\chi_{j'\sigma'})} + 2\frac{\partial \overline{\mathcal{W}}}{\partial(i\chi_{j\sigma})} \mathcal{R} \frac{\partial \overline{\mathcal{W}}}{\partial(i\chi_{j'\sigma'})} + 2\frac{\partial \overline{\mathcal{W}}}{\partial(i\chi_{j'\sigma'})} \mathcal{R} \frac{\partial \overline{\mathcal{W}}}{\partial(i\chi_{j\sigma})} \right. \right. \right.$$
$$+ \langle\!\langle I_{j\sigma} \rangle\!\rangle \left[\frac{\partial^2 \overline{\mathcal{W}}}{\partial(i\chi_{j'\sigma'})\partial z} + 2\frac{\partial \overline{\mathcal{W}}}{\partial(i\chi_{j'\sigma'})} \mathcal{R} \frac{\partial \overline{\mathcal{W}}}{\partial z} + 2\frac{\partial \overline{\mathcal{W}}}{\partial z} \mathcal{R} \frac{\partial \overline{\mathcal{W}}}{\partial(i\chi_{j'\sigma'})} \right]$$
$$\left. \left. + \langle\!\langle I_{j'\sigma'} \rangle\!\rangle \left[\frac{\partial^2 \overline{\mathcal{W}}}{\partial(i\chi_{j\sigma})\partial z} + 2\frac{\partial \overline{\mathcal{W}}}{\partial(i\chi_{j\sigma})} \mathcal{R} \frac{\partial \overline{\mathcal{W}}}{\partial z} + 2\frac{\partial \overline{\mathcal{W}}}{\partial z} \mathcal{R} \frac{\partial \overline{\mathcal{W}}}{\partial(i\chi_{j\sigma})} \right] \right\} \right| 0 \right\rangle\!\!\right\rangle_{\{\boldsymbol{\chi}_{j\sigma}\} \to \{\mathbf{0}\}, z \to 0}. \tag{26}$$

The total charge and spin current noise can be obtained utilizing Eq. (19). Moreover, higher-order cumulants can be obtained recursively in a similar manner.

Different from the results for charge current cumulants [53,54], higher-order spin-resolved cumulants apparently involve correlations between different spin currents; see for

instance, $\langle\langle I_{j\sigma} I_{j'\sigma'}\rangle\rangle$ in Eq. (26). These correlations may have vital roles to play in spin-dependent transport. An essential effect is that these spin-dependent correlations could exist even though the net charge current is zero, as we will show in the following section for symmetric tunnel couplings of up and down spins. Furthermore, for the case of very asymmetric spin tunnel couplings, these spin-dependent correlations are found to be responsible for an anomalous feature between autocorrelations and cross correlations: A super-Poissonian autocorrelation is observed despite a negative cross correlation and a positive cross correlation occurs with a sub-Poissoianian autocorrelation.

We have presented a generic approach for the calculation of the spin-resolved counting statistics in the presence of non-Markovian memory effects. Although the formalism has been developed in the context of an ESR-based three-terminal QD system, it is applicable to a wide range of spin transport systems. Furthermore, the approach allows us to obtain, in principle, any order of spin-resolved cumulants in a recursive manner.

V. RESULTS AND DISCUSSION

In this section, we present the spin-resolved non-Markovian noise characteristics in both cases of symmetric and strongly asymmetric spin tunnel couplings, where some universal noise results for charge and spin currents and anomalous features between autocorrelations and cross correlations will be revealed. Finite-frequency spin-resolved noise is also investigated in the non-Markovian regime based on the Mac-Donald's formula. Transition from coherence to incoherence will be demonstrated clearly in the noise spectrum.

A. Symmetric spin tunnel couplings

The first cumulants are related to spin currents through junction j. For symmetric spin tunnel couplings ($\Gamma_{j\sigma} = \Gamma$), they are simply given by

$$\langle\langle I_{j\downarrow}\rangle\rangle = -\langle\langle I_{j\uparrow}\rangle\rangle = \frac{\Gamma\gamma_0^+}{3\Gamma + \gamma_0^- + 2\gamma_0^+}. \tag{27}$$

In this case, electrons with up and down spins tunnel into and out of each electrode with equivalent rates. According to Eq. (17), the total charge current in electrode j is
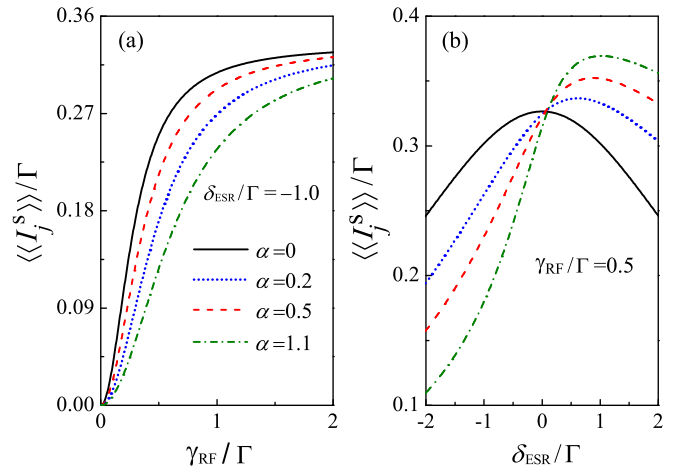

FIG. 2. The spin current through junction j as a function of (a) the magnitude and (b) the ESR detuning of the driving field with different dissipation strengths α. The tunnel couplings are symmetric, i.e., $\Gamma_{j\sigma} = \Gamma$. The other parameters are heat bath temperature $T = 0$ and high-energy cutoff $\omega_c = 100\Gamma$.

exactly zero $\langle\langle I_j^c\rangle\rangle = \langle\langle I_{j\downarrow}\rangle\rangle + \langle\langle I_{j\uparrow}\rangle\rangle = 0$ and the total spin current through electrode j is given by $\langle\langle I_j^s\rangle\rangle = \langle\langle I_{j\downarrow}\rangle\rangle - \langle\langle I_{j\uparrow}\rangle\rangle = 2\langle\langle I_{j\downarrow}\rangle\rangle$.

The numerical results for $\langle\langle I_j^s\rangle\rangle$ versus γ_{RF} are displayed in Fig. 2(a) for various values of α. The value of $\langle\langle I_j^s\rangle\rangle$ is proportional to the excitation power ($\langle\langle I_j^s\rangle\rangle \propto \gamma_{RF}^2$), which is consistent with the prototype of the present ESR pumping device. As γ_{RF} increases, $\langle\langle I_j^s\rangle\rangle$ saturates regardless of value of α, which is also implied in Eq. (27). The effect of phonon absorption and emission is essentially reflected in Fig. 2(b), where $\langle\langle I_j^s\rangle\rangle$ is plotted versus δ_{ESR}. Without coupling to the heat bath ($\alpha = 0$), $\langle\langle I_j^s\rangle\rangle$ is symmetric about $\delta_{ESR} = 0$, whereas asymmetry is observed in the presence of finite coupling to the heat bath. The asymmetry arises due to the asymmetric emission and absorption of phonons, where, at low temperatures and for $\delta_{ESR} < 0$, phonon absorption dominates, and $\langle\langle I_j^s\rangle\rangle$ is suppressed. In the opposite regime of $\delta_{ESR} > 0$, the phonon emission process is dominant, leading to an enhancement in $\langle\langle I_j^s\rangle\rangle$.

The second cumulants are directly related to the spin-resolved shot noise. Utilizing Eq. (26), the spin-resolved cumulants reflecting autocorrelation for electrode j are given by

$$\langle\langle I_{j\sigma} I_{j\sigma}\rangle\rangle = +|\langle\langle I_{j\sigma}\rangle\rangle|\left\{1 + \frac{6\Gamma(\gamma_0^- \dot{\gamma}_0^+ - \gamma_0^+ \dot{\gamma}_0^-) + 6\Gamma(3\Gamma\dot{\gamma}_0^+ - 2\gamma_0^+) - 2\gamma_0^+(\gamma_0^+ + \gamma_0^-)}{3(3\Gamma + \gamma_0^- + 2\gamma_0^+)^2}\right\}, \tag{28a}$$

$$\langle\langle I_{j\sigma} I_{j\bar{\sigma}}\rangle\rangle = -|\langle\langle I_{j\sigma}\rangle\rangle|\left\{\frac{1}{3} + \frac{6\Gamma(\gamma_0^- \dot{\gamma}_0^+ - \gamma_0^+ \dot{\gamma}_0^-) + 6\Gamma(3\Gamma\dot{\gamma}_0^+ - 2\gamma_0^+) - 2\gamma_0^+(\gamma_0^+ + \gamma_0^-)}{3(3\Gamma + \gamma_0^- + 2\gamma_0^+)^2}\right\}, \tag{28b}$$

where we have employed the notation $\dot{\gamma}_0^\pm \equiv \partial_z \gamma_z^\pm|_{z\to 0}$ and $\bar{\sigma} = -\sigma$. Analogously, the spin-resolved cumulants reflecting cross correlations between different electrodes are obtained as

$$\langle\langle I_{j\sigma} I_{j'\sigma}\rangle\rangle = \langle\langle I_{j\sigma} I_{j\sigma}\rangle\rangle - |\langle\langle I_{j\sigma}\rangle\rangle| \quad (j \neq j'), \tag{29a}$$

$$\langle\langle I_{j\sigma} I_{j'\bar{\sigma}}\rangle\rangle = \langle\langle I_{j\sigma} I_{j\bar{\sigma}}\rangle\rangle, \quad (j \neq j'). \tag{29b}$$

From Eqs. (28) and (29), one readily obtains the autocorrelations of the net charge current [Eq. (19a)]

$$\langle\langle I_j^c I_j^c\rangle\rangle = \frac{2}{3}|\langle\langle I_j^s\rangle\rangle|, \tag{30}$$

as well as the cross correlations between different electrodes

$$\langle\langle I_j^c I_{j'}^c\rangle\rangle = -\frac{1}{3}|\langle\langle I_j^s\rangle\rangle| \quad (j \neq j'), \tag{31}$$

which are universal results, regardless of the values δ_{ESR}, γ_{RF} and α. Furthermore, Eqs. (30) and (31) unambiguously demonstrate that the spin pumping process does generate charge current shot noise even though, according to Eq. (17a), the net charge current $\langle\langle I_j^c \rangle\rangle$ is zero. Generally, shot noise occurs when a quantum system is driven out of equilibrium. Our results therefore reveal that such nonequilibrium shot noise can occur even when no bias is applied. In this case, the oscillating magnetic field acts as effective bias voltage. Equations (30) and (31) also demonstrate that the resultant charge current shot noise is intimately related to $\langle\langle I_j^s \rangle\rangle$, rather than $\langle\langle I_j^c \rangle\rangle$. The cross correlation in Eq. (31) is negative definite, indicating an antibunching behavior for transported quasiparticles. The corresponding autocorrelation is thus below the Poissonian value, i.e., it represents sub-Poissonian noise, consistent with the arguments in Refs. [1,13].

It is also instructive to investigate the shot noise of the total spin current according to Eq. (19b). The spin current noise has been shown to be capable of detecting attractive or repulsive interactions [62] and revealing a dynamical spin blockade mechanism [63]. Furthermore, analogous to the charge current shot noise, which can be used to measure the charge of quasiparticles in a tunneling process [64–70], the spin current shot noise may serve as a transparent means of determining the spin unit of a quasiparticle that has been transported through the device. Let us focus on the case of $\delta_{\text{ESR}} = 0$ and $\alpha = 0$. The autocorrelations and cross correlations of $\langle\langle I_j^s \rangle\rangle$ are given, respectively, by

$$\frac{\langle\langle I_j^s I_j^s \rangle\rangle}{|\langle\langle I_j^s \rangle\rangle|} = \frac{4}{3}\left\{1 - \frac{2\eta(3+\eta)}{(2+3\eta)^2}\right\}, \tag{32a}$$

$$\frac{\langle\langle I_j^s I_{j'}^s \rangle\rangle}{|\langle\langle I_j^s \rangle\rangle|} = \frac{1}{3}\left\{1 - \frac{8\eta(3+\eta)}{(2+3\eta)^2}\right\} \quad (j \neq j'), \tag{32b}$$

with $\eta = (2\gamma_{\text{RF}}/3\Gamma)^2$. Interestingly, in the limit of small η, the autocorrelations and cross correlations of spin currents are reduced to $\langle\langle I_j^s I_j^s \rangle\rangle/|\langle\langle I_j^s \rangle\rangle| \rightarrow \frac{4}{3}$ and $\langle\langle I_j^s I_{j'}^s \rangle\rangle/|\langle\langle I_j^s \rangle\rangle| \rightarrow \frac{1}{3}$, respectively. These results imply another universal regime, where both autocorrelations and cross correlations of $\langle\langle I_j^s \rangle\rangle$ determine the spin unit of a quasiparticle transported through the device, and their ratio is universally 4.

We have now presented both autocorrelations and cross correlations of charge and spin currents for symmetric spin tunnel couplings. In this case, up and down spins tunnel, respectively, into and out of QD with the same rate. Yet, both charge and spin current noises are uniquely associated with the spin current, reflecting the fact that the fluctuations in spin current could also give rise to a charge current noise even though the net charge current is zero. We further reveal that the correlations between opposite spin currents have essential roles to play for both spin and charge current noises to reach their universal results. These universal results may provide a crucial means of measuring the charge and spin of quasiparticles in a mesoscopic spin transport system.

B. Strongly asymmetric spin tunnel couplings

We are now in a position to discuss noise cumulants in the opposite limit of very asymmetric spin tunneling rates.
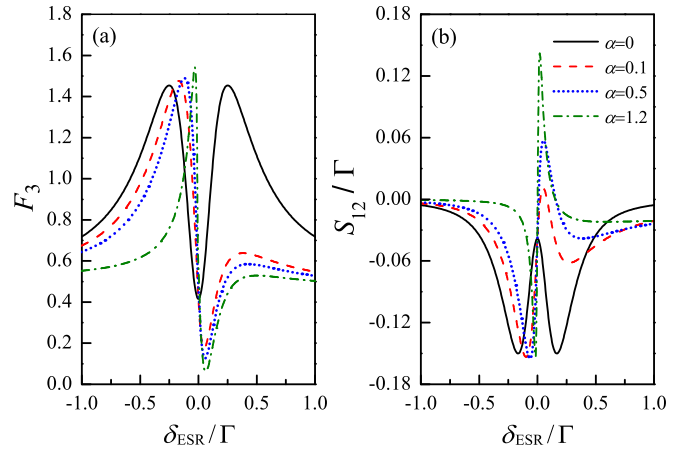

FIG. 3. (a) Autocorrelation, expressed as the Fano factor $F_3 \equiv \langle\langle (I_3^c)^2 \rangle\rangle/\langle\langle I_3^s \rangle\rangle$, and (b) cross correlation of the charge current versus δ_{ESR} for very asymmetric spin tunneling rates: $\Gamma_{1\uparrow} = \Gamma_{2\uparrow} = \Gamma_{3\downarrow} = \frac{3}{10}\Gamma$, and $\Gamma_{1\downarrow} = \Gamma_{2\downarrow} = \Gamma_{3\uparrow} = \frac{1}{30}\Gamma$. The other parameters are $\gamma_{\text{RF}} = 0.5\Gamma$, $T = 0$, and $\omega_c = 100\Gamma$.

Asymmetry in spin-dependent tunnel couplings may arise in normal electrodes due to spin-orbital coupling [71–74] or different electron g factors in the electrode and in the QD [75,76], or in ferromagnetic electrodes due to different densities of states for majority and minority electrons [77]. In the following discussion, we will reveal an important new aspect of the present work. That is an anomalous relation between autocorrelations and cross correlations: A super-Poissonian autocorrelation is observed with a negative cross correlation, while a positive cross correlation occurs in spite of a sub-Poissonian autocorrelation.

The autocorrelations and cross correlations of the charge current for various values of α are plotted in Figs. 3(a) and 3(b), respectively, with strongly asymmetric spin-dependent tunneling rates: $\Gamma_{1\uparrow} = \Gamma_{2\uparrow} = \Gamma_{3\downarrow} = \frac{3}{10}\Gamma$ and $\Gamma_{1\downarrow} = \Gamma_{2\downarrow} = \Gamma_{3\uparrow} = \frac{1}{30}\Gamma$. In this case, the dominant transport process involves a spin-up electron tunneling from either electrode 1 or 2 into the QD, where its spin is flipped prior to tunneling out to electrode 3. It is observed for $\alpha = 0$ [the solid line in Fig. 3(a)] that the autocorrelation, expressed as the Fano factor $F_3 \equiv \langle\langle (I_3^c)^2 \rangle\rangle/\langle\langle I_3^c \rangle\rangle$, exhibits unambiguously super-Poissonian characteristics in the regime close to $\delta_{\text{ESR}}/\Gamma = \pm\frac{1}{4}$. However, as shown by the solid line in Fig. 3(b), the corresponding cross correlation $S_{12} = \langle\langle I_1^c I_2^c \rangle\rangle$ between electrodes 1 and 2 is clearly negative.

With finite coupling to the heat bath, asymmetric correlations are observed due to asymmetry in the emission and absorption of bosons at low temperatures. In the regime $\delta_{\text{ESR}} < 0$, neither the autocorrelation nor the cross correlation is sensitive to the value of α. In the opposite regime of $\delta_{\text{ESR}} > 0$, however, the correlations are significantly affected by the value of α, and, as α increases, the autocorrelation F_3 is reduced from a super-Poissonian to a sub-Poissonian value. However, S_{12} is correspondingly enhanced unambiguously from a negative to a positive value. Remarkably, a positive cross correlation is observed in the absence of a super-Poissonian autocorrelation.
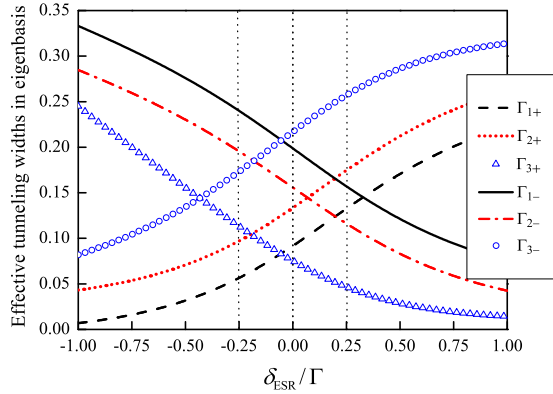
FIG. 4. Effective tunneling widths through eigenstates $|\pm\rangle$ versus ESR detuning for $\Gamma_{1\uparrow} = \Gamma_{2\uparrow} = \Gamma_{3\downarrow} = \frac{3}{10}\Gamma$, and $\frac{1}{3}\Gamma_{1\downarrow} = \Gamma_{2\downarrow} = \frac{1}{5}\Gamma_{3\uparrow} = \frac{1}{90}\Gamma$. Other parameters are the same as those in Fig. 3.

In order to explore the underlying physics responsible for the occurrence of the anomalous feature between autocorrelations and cross correlations, we first diagonalize the reduced system Hamiltonian [Eq. (3)] as

$$\tilde{\mathcal{H}}_{\mathrm{QD}} = \frac{1}{2}\tilde{\Delta}\{|+\rangle\langle+| - |-\rangle\langle-|\}, \tag{33}$$

with $\tilde{\Delta} = \sqrt{\delta_{\mathrm{ESR}}^2 + 4\gamma_{\mathrm{RF}}^2}$. Spin tunneling through the QD then can be mapped onto transport through a parallel two-level system. The involved eigenstates are given, respectively, by

$$|+\rangle = \sin\frac{\Theta}{2}|\uparrow\rangle - \cos\frac{\Theta}{2}|\downarrow\rangle, \tag{34a}$$

$$|-\rangle = \cos\frac{\Theta}{2}|\uparrow\rangle + \sin\frac{\Theta}{2}|\downarrow\rangle, \tag{34b}$$

where Θ is introduced via $\sin\Theta = 2\gamma_{\mathrm{RF}}/\tilde{\Delta}$ and $\cos\Theta = \delta_{\mathrm{ESR}}/\tilde{\Delta}$. As a result, the system-electrode tunnel-coupling Hamiltonian in Eq. (5) is recast as

$$\tilde{H}_{\mathrm{QD-el}} = \sum_{j,k} \sum_{s=+,-} \{t_{jk}^{(s)} c_{jks}^\dagger |0\rangle\langle s| + \mathrm{H.c.}\}, \tag{35}$$

where the effective tunneling amplitudes through eigenstates $|+\rangle$ and $|-\rangle$ are given by $t_{jk}^{(+)} = t_{jk\uparrow}\sin(\frac{\Theta}{2}) - t_{jk\downarrow}\cos(\frac{\Theta}{2})$ and $t_{jk}^{(-)} = t_{jk\uparrow}\cos(\frac{\Theta}{2}) + t_{jk\downarrow}\sin(\frac{\Theta}{2})$, respectively. The corresponding tunneling widths $\Gamma_{js} = 2\pi\sum_k |t_{jk}^{(s)}|^2\delta(\omega - \epsilon_{jks})$ therefore sensitively depend on δ_{ESR}. To clearly elucidate the physical insight responsible for the anomalous noise feature, we now discuss the correlations for the following five typical values of ESR detunings: (i) $\delta_{\mathrm{ESR}} = 0$, (ii) $\delta_{\mathrm{ESR}} = -\Gamma$, (iii) $\delta_{\mathrm{ESR}} = \Gamma$, (iv) $\delta_{\mathrm{ESR}} = -\frac{1}{4}\Gamma$, and (v) $\delta_{\mathrm{ESR}} = \frac{1}{4}\Gamma$. The corresponding values of Γ_{js} can be found in Fig. 4.

(i) $\delta_{\mathrm{ESR}} = 0$. In this case, electrons tunneling through the eigenstate $|-\rangle$ dominates; see Fig. 4. The system resembles the case of transport through a single-level system with approximately symmetric tunneling rates. The autocorrelation is sub-Poissonian and the corresponding cross correlation is negative [see Fig. 3].

(ii) $\delta_{\mathrm{ESR}}/\Gamma = -1$. It is found from Fig. 4 that Γ_{1-}, Γ_{2-}, and Γ_{3+} dominate. An electron tunnels from electrode 1 or 2 into state $|-\rangle$, where it may reside for a long time before it is excited to state $|+\rangle$ by absorbing energy quanta from the phonon bath,
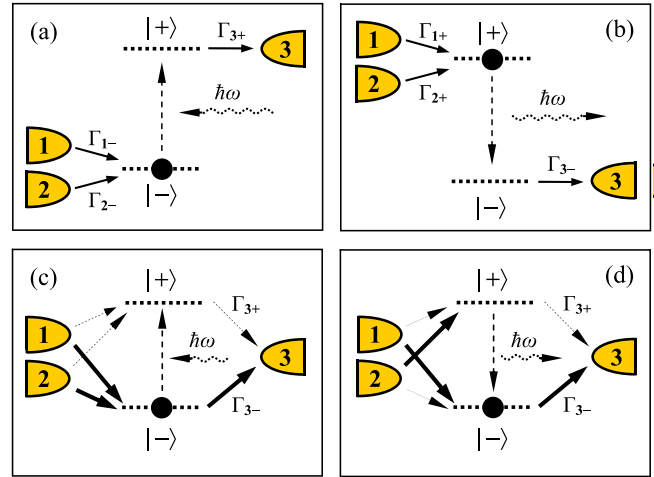
and, eventually, tunnels out to electrode 3, as schematically illustrated in Fig. 5(a). The system can be mapped to a serial double QD in the sequential tunneling regime [78], and thus the autocorrelation is below the Poissonian value and the cross correlation is negative.

(iii) $\delta_{\mathrm{ESR}}/\Gamma = 1$. Analogous to the case of (ii) but the rates Γ_{1+}, Γ_{2+}, and Γ_{3-} are now dominant. As shown in Fig. 5(b), an electron flows into state $|+\rangle$ through electrode 1 or 2, relaxes to state $|-\rangle$ with phonon emission, and eventually tunnels out to electrode 3. Again, the transport can be mapped to that of a serial double QD, and thus the noise characteristics are qualitatively similar to those in the case (ii).

(iv) $\delta_{\mathrm{ESR}} = -\frac{1}{4}\Gamma$. For this moderate value of ESR detuning, an electron respectively tunnels into and out of state $|-\rangle$ with characteristic times $(\Gamma_{1-} + \Gamma_{2-})^{-1}$ and $(\Gamma_{3-})^{-1}$ are rapid in comparison with those through state $|+\rangle$, i.e., $(\Gamma_{1+} + \Gamma_{2+})^{-1}$ and $(\Gamma_{3+})^{-1}$, indicative of fast $(|-\rangle)$ and slow $(|+\rangle)$ channels [see Figs. 4 and 5(c)]. In the presence of strong Coulomb interactions that prevent double occupancy on the QD, electron transport competes between these two channels, where the fast flow of electrons through state $|-\rangle$ is modulated by slow transport through state $|+\rangle$. The fast-to-slow mechanism [26,51,63,78–81] leads to the bunching of tunneling events, and, eventually, to the super-Poissonian characteristics shown in Fig. 3(a). Moreover, super-Poissonian noise is even slightly increased with rising α. This is due to the fact that the phonon absorption process dominates for $\delta_{\mathrm{ESR}} < 0$ [cf. Fig. 5(c)], which may excite an electron from the fast channel to the slow channel, and, thus, further enhance the fast-to-slow mechanism.

(v) $\delta_{\mathrm{ESR}} = \frac{1}{4}\Gamma$. As schematically shown in Fig. 5(d), an electron tunnels into eigenstates $|+\rangle$ and $|-\rangle$ with comparable rates $(\Gamma_{1+} + \Gamma_{2+} \simeq \Gamma_{1-} + \Gamma_{2-})$ but leaves the QD with quite different rates $(\Gamma_{3-} \gg \Gamma_{3+})$. Without coupling to the phonon bath $(\alpha = 0)$, the fast-to-slow mechanism still exists, which leads to the bunching of tunneling events and super-Poissonian noise, as shown in Fig. 3(a). Yet, under the condition of finite coupling to the phonon bath, an electron trapped in the slow
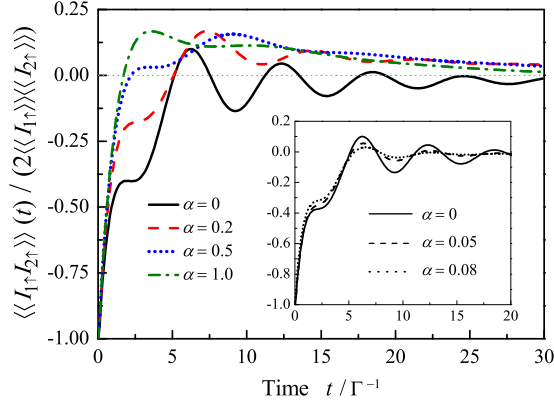

FIG. 5. Dominant tunneling processes in the eigenstate representation corresponding to different values of δ_{ESR}: (a) $\delta_{\mathrm{ESR}} = -\Gamma$, (b) $\delta_{\mathrm{ESR}} = \Gamma$, (c) $\delta_{\mathrm{ESR}} = -\Gamma/4$, and (d) $\delta_{\mathrm{ESR}} = \Gamma/4$. All other parameters are equivalent to those employed in Fig. 3.

FIG. 6. Time correlation function component $\langle\langle I_{1\uparrow} I_{2\uparrow} \rangle\rangle(t)$ for $\delta_{\mathrm{ESR}}/\Gamma = 0.08$ with different values of α. All other parameters are equivalent to those employed in Fig. 3. The inset shows the results in the Markovian limit for weak dissipation strength.

channel $|+\rangle$ may relax to the fast channel $|-\rangle$, and then tunnel out to electrode 3; see Fig. 5(d). The fast-to-slow mechanism is thus lifted, which explains the reduction of the autocorrelation F_3 in Fig. 3(a).

Now let us investigate the sign reversal (from negative to positive) of the cross correlation S_{12} via analyzing the corresponding time correlation function $\langle\langle I_1^c I_2^c \rangle\rangle(t)$. In the case of $\delta_{\mathrm{ESR}} = \frac{1}{4}\Gamma$, the primary contribution derives from the spin-resolved component $\langle\langle I_{1\uparrow} I_{2\uparrow} \rangle\rangle(t)$, which is evaluated according to the quantum jump theory [82]. The numerical results are displayed in Fig. 6 for different values of α. In the sequential tunneling limit, spins tunnel through the device one by one. It implies $\lim_{t\to 0^+}\langle\langle I_{1\uparrow} I_{2\uparrow} \rangle\rangle(t) = -2\langle\langle I_{1\uparrow} \rangle\rangle \langle\langle I_{2\uparrow} \rangle\rangle$, independent of α; see also Fig. 6. For finite times, $\langle\langle I_{1\uparrow} I_{2\uparrow} \rangle\rangle(t)$ depends sensitively on the α. Without coupling to the heat bath, the system maintains its coherence for a long time, cf. the solid curve in Fig. 6. With increasing α, the system loses its coherence rapidly due to coupling with the heat bath; see, for instance, the dash-dotted curve for $\alpha = 1.0$ in Fig. 6.

The typical time scales in $\langle\langle I_{1\uparrow} I_{2\uparrow} \rangle\rangle(t)$ involve the average delay between the occupancy of the dot by two consecutive up electrons $\tau_0 = \varrho_{00}^{\mathrm{st}}/\sum_j S_j^{\mathrm{Sch}}$ and the average dwell time of spin-σ electrons on the QD $\tau_\sigma = \varrho_{\sigma\sigma}^{\mathrm{st}}/\sum_j S_{j\sigma}^{\mathrm{Sch}}$, where $S_{j\sigma}^{\mathrm{Sch}} = 2\langle\langle I_{j\sigma} \rangle\rangle$ is the Schottky noise associated with the tunneling of spin-σ electrons through junction j, and $S_j^{\mathrm{Sch}} = \sum_\sigma S_{j\sigma}^{\mathrm{Sch}}$ [52,63]. Let us focus on the situation of a strong dissipation strength with $\alpha = 1.0$; see the dash-dotted curve in Fig. 6. The time correlation is negative for $t < \tau_0 \approx 1.7\Gamma^{-1}$. It then increases, becomes positive, and attains a maximum value at approximately $t = \tau_\uparrow \approx 3.6\Gamma^{-1}$. Finally, it decreases on a time scale of $t = \tau_\uparrow + \tau_\downarrow \approx 16.5\Gamma^{-1}$. In comparison, these unique time features are not identified in case of Markovian limit and weak system-bath coupling, cf. inset of Fig. 6. It thus allows us to attribute the observed positive S_{12} to the non-Markovian influence due to strong coupling between the system and the heat bath.

C. Non-Markovian finite-frequency noise

Now we are in a position to investigate the second new aspect of the present work, which is the finite-frequency
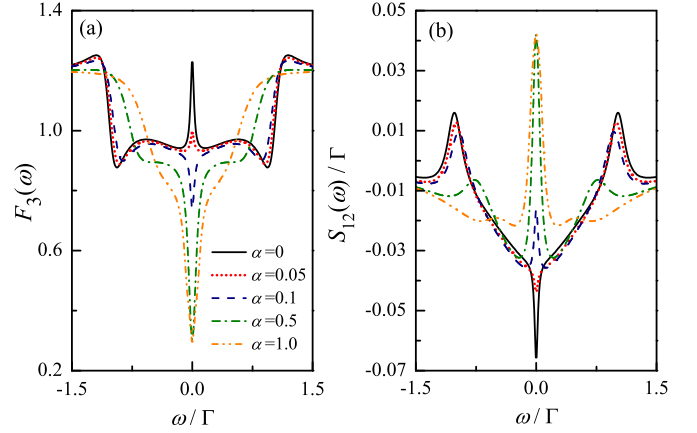

FIG. 7. Finite-frequency noise autocorrelation $F_3(\omega)$ and cross correlation $S_{12}(\omega)$ for $\delta_{\mathrm{ESR}}/\Gamma = 0.08$ with different α. All other parameters are equivalent to those employed in Fig. 3.

noise in the non-Markovian regime. Recently, accurate noise measurements on all relevant frequencies have been enabled using a nearby quantum point contact for on-chip real-time detection of current pulses in single-electron devices [83,84]. Here, the second cumulant of the spin current is of primary interest, and its symmetrized finite-frequency current noise can be expressed by MacDonald's formula as [85]

$$S_{j\sigma,j'\sigma'}(\omega) = \omega \int_0^\infty dt\, \sin(\omega t)\langle\langle I_{j\sigma} I_{j'\sigma'} \rangle\rangle(t), \qquad (36)$$

where $\langle\langle I_{j\sigma} I_{j'\sigma'} \rangle\rangle(t) = \frac{d}{dt}\frac{\partial^2 \mathcal{F}(\{\chi_{j\sigma}\},t)}{\partial(\mathrm{i}\chi_{j\sigma})\partial(\mathrm{i}\chi_{j'\sigma'})}|_{\{\chi_{j\sigma}\}\to\{\mathbf{0}\}}$, for $\mathcal{F}(\{\chi_{j\sigma}\},t)$ given by Eq. (15). Eventually, one arrives at

$$S_{j\sigma,j'\sigma'}(\omega) = -\frac{\omega^2}{2}\frac{\partial^2}{\partial(\mathrm{i}\chi_{j\sigma})\partial(\mathrm{i}\chi_{j'\sigma'})}[\langle\mathcal{G}(\{\chi_{j\sigma}\},z = +\mathrm{i}\omega)\rangle$$
$$+ \langle\mathcal{G}(\{\chi_{j\sigma}\},z = -\mathrm{i}\omega)\rangle]|_{\{\chi_{j\sigma}\}\to\{\mathbf{0}\}}, \qquad (37)$$

where $\langle\mathcal{G}(\{\chi_{j\sigma}\},z)\rangle = \mathrm{tr}\{\mathcal{G}(\{\chi_{j\sigma}\},z)[\varrho(\{\chi_{j\sigma}\},t=0)+\tilde{\Upsilon}(z)]\}$. The evaluation of the above expression requires an appropriate treatment of the initial condition, as given by Eq. (A12). It implies the essential roles that inhomogeneity may play in the finite-frequency cumulant. Moreover, an appropriate inclusion of the inhomogeneity guarantees a correct finite-time behavior, i.e., the proper normalization of the reduced density matrix at all times ($\mathrm{tr}\{\varrho(t)\} = 1$). With the knowledge of the individual spin-resolved noise components in Eq. (37), the total noise spectrum is obtained according to Eq. (19).

The finite-frequency autocorrelations and cross correlations of the charge currents are presented in Fig. 7 for different values of α. Near $\omega = 0$, F_3 crosses from a super-Poissonian to a sub-Poissonian value and S_{12} undergoes a sign reversal from negative to positive as α increases, consistent with the results in Fig. 3. The dips located approximately at frequencies $\tilde{\Delta} = \sqrt{\delta_{\mathrm{ESR}}^2 + 4\gamma_{\mathrm{RF}}^2}$ in both the autocorrelations and cross correlations directly reflect the resonance between the two quantum spin states. Coupling to the phonon bath renormalizes the eigenspectrum of the spin degrees of freedom, such that the resonances are shifted toward lower frequencies. The half width of the resonant peak around $\omega = \tilde{\Delta}$ may be utilized as an essential tool to extract the total dephasing rate of the

spin system due to coupling with both electronic reservoirs and a heat bath [86]. As α increases, the resonance signatures are washed out, indicating how the coherent dynamics of the system gets progressively damped by the phonon bath.

VI. SUMMARY

We investigated noise correlations in an electron spin resonance-pumped three-terminal single quantum dot system. A recursive scheme was employed for the calculation of the spin-resolved counting statistics in the presence of non-Markovian effects due to strong coupling to a dissipative heat bath. We demonstrated for symmetric tunneling rates of up and down spins that the ESR pumping process universally generated both charge and spin current shot noises despite the condition of a zero charge current, which provides a practical method for measuring quasiparticle charge and spin in mesoscopic transport. In the opposite limit of very asymmetric spin tunneling rates, an anomalous relation between noise autocorrelations and cross correlations was revealed in the regime $\delta_{\text{ESR}} > 0$ due to complicated phonon-assisted hopping processes and non-Markovian memory effects. Here, super-Poissonian autocorrelation was observed in spite of a negative cross correlation. Moreover, with increasing α, the charge current autocorrelation was strongly suppressed from a super-Poissonian to a sub-Poissonian value while the corresponding cross correlation underwent a sign reversal from negative to positive. These unique noise features may offer essential methods for exploiting internal spin dynamics and various quasiparticle tunneling processes in the study of mesoscopic transport. The experimental verification of these predictions is greatly anticipated in the near future.

ACKNOWLEDGMENTS

APPENDIX A: DERIVATION OF THE NON-MARKOVIAN SPIN-RESOLVED QME

The spin dynamics of the reduced system conditioned on the number of tunneled spins is described by the $\{N_{j\sigma}\}$-resolved QME. By introducing the spin-resolved counting fields $(\{\chi_{j\sigma}\}) = (\chi_{1\uparrow}, \chi_{1\downarrow}, \chi_{2\uparrow}, \chi_{2\downarrow}, \chi_{3\uparrow}, \chi_{3\downarrow})$ associated with the numbers of tunneled spin $(\{N_{j\sigma}\})$, the $\{N_{j\sigma}\}$-resolved QME is recast to a counting-field-resolved QME for $\rho(\{\chi_{j\sigma}\}, t)$. Under the second-order expansion of the tunnel coupling and partial tracing over the degrees of freedom of the electrodes, the counting-field-dressed QME reads

$$\frac{\partial}{\partial t}\rho(\{\chi_{j\sigma}\}, t) = \mathcal{L}(\{\chi_{j\sigma}\})\rho(t) - i[H_{\text{B}} + F_{\text{B}}Q_z, \rho(\{\chi_{j\sigma}\}, t)],$$
(A1)

where the first term $\mathcal{L}(\{\chi_{j\sigma}\})$ describes spin-dependent tunneling through the electrodes and the second term accounts for the effect of dissipative phonon bath.

Specifically, let us consider the occupation state representation $(|0\rangle, |\uparrow\rangle, |\downarrow\rangle)$ (cf. Fig. 1), in which the reduced density matrix is denoted as $\rho = (\rho_{00}, \rho_{\uparrow\uparrow}, \rho_{\downarrow\downarrow}, \rho_{\uparrow\downarrow}, \rho_{\downarrow\uparrow})^{\text{T}}$. Here, ρ_{00} and $\rho_{\sigma\sigma}$ describe the occupation probability in the QD being, respectively, empty and spin-σ ($\sigma = \uparrow, \downarrow$) states, and the off-diagonal terms $\rho_{\uparrow\downarrow}$ and $\rho_{\downarrow\uparrow}$ stand for coherent superposition of up- and down-spin states. The corresponding counting-field-dressed QME (A1) reads

$$\dot{\rho}_{00} = -\tilde{\Gamma}_{\uparrow}^0 \rho_{00} + \tilde{\Gamma}_{\downarrow}^{\chi_\downarrow} \rho_{\downarrow\downarrow} - i[H_{\text{B}}, \rho_{00}],$$
(A2a)

$$\dot{\rho}_{\uparrow\uparrow} = i\gamma_{\text{RF}}(\rho_{\uparrow\downarrow} - \rho_{\downarrow\uparrow}) + \tilde{\Gamma}_{\uparrow}^{\chi_\uparrow}\rho_{00} - i[H_{\text{B}} + F_{\text{B}}, \rho_{\uparrow\uparrow}],$$
(A2b)

$$\dot{\rho}_{\downarrow\downarrow} = i\gamma_{\text{RF}}(\rho_{\downarrow\uparrow} - \rho_{\uparrow\downarrow}) - \tilde{\Gamma}_{\downarrow}^0 \rho_{\downarrow\downarrow} - i[H_{\text{B}} - F_{\text{B}}, \rho_{\downarrow\downarrow}],$$
(A2c)

$$\dot{\rho}_{\uparrow\downarrow} = -\frac{1}{2}\tilde{\Gamma}_{\downarrow}^0 \rho_{\uparrow\downarrow} - i\delta_{\text{ESR}}\rho_{\uparrow\downarrow} + i\gamma_{\text{RF}}(\rho_{\uparrow\uparrow} - \rho_{\downarrow\downarrow})$$
$$\quad - i[H_{\text{B}}, \rho_{\uparrow\downarrow}] - i\{F_{\text{B}}, \rho_{\uparrow\downarrow}\},$$
(A2d)

$$\dot{\rho}_{\downarrow\uparrow} = -\frac{1}{2}\tilde{\Gamma}_{\downarrow}^0 \rho_{\downarrow\uparrow} + i\delta_{\text{ESR}}\rho_{\downarrow\uparrow} - i\gamma_{\text{RF}}(\rho_{\uparrow\uparrow} - \rho_{\downarrow\downarrow})$$
$$\quad - i[H_{\text{B}}, \rho_{\downarrow\uparrow}] + i\{F_{\text{B}}, \rho_{\downarrow\uparrow}\},$$
(A2e)

where $\tilde{\Gamma}_{\sigma}^{\chi_\sigma} = \sum_{j=1,2,3} \Gamma_{j\sigma} e^{i\chi_{j\sigma}}$ is the counting-field-dressed tunneling width for a spin-σ electron and the curly brackets $\{X, Y\} = XY + YX$ stands for the anticommutator.

It should be noted that in deriving Eq. (A1) only the degrees of freedom of the electrodes have been traced out, matrix elements $\rho_{\sigma\sigma'}$ are still operators in the Hilbert space of the boson bath. The next step is to trace out the degrees of the freedom of the phonon bath to obtain the dynamics of the reduced system alone, i.e., $\varrho_{\sigma\sigma'} = \text{tr}_{\text{B}}\{\rho_{\sigma\sigma'}\}$, with $\text{tr}_{\text{B}}\{\cdots\}$ the trace over the bosonic degrees of freedom. The dynamics for the occupation probabilities are readily given by

$$\dot{\varrho}_{00} = -\tilde{\Gamma}_{\uparrow}^0 \varrho_{00} + \tilde{\Gamma}_{\downarrow}^{\chi_\downarrow} \varrho_{\downarrow\downarrow},$$
(A3a)

$$\dot{\varrho}_{\uparrow\uparrow} = \tilde{\Gamma}_{\uparrow}^{\chi_\uparrow} \varrho_{00} + i\gamma_{\text{RF}}\text{tr}_{\text{B}}\{(\rho_{\uparrow\downarrow} - \rho_{\downarrow\uparrow})\},$$
(A3b)

$$\dot{\varrho}_{\downarrow\downarrow} = -\tilde{\Gamma}_{\downarrow}^0 \varrho_{\downarrow\downarrow} - i\gamma_{\text{RF}}\text{tr}_{\text{B}}\{(\rho_{\uparrow\downarrow} - \rho_{\downarrow\uparrow})\}.$$
(A3c)

The effect of the phonon bath on spin dynamics is thus fully incorporated through the off-diagonal elements $\rho_{\uparrow\downarrow}$ and $\rho_{\downarrow\uparrow}$. From Eqs. (A2d) and (A2e), their solutions formally read

$$\rho_{\uparrow\downarrow}(t) = i\gamma_{\text{RF}} \int_0^t d\tau\, e^{-\xi_+(t-\tau)} e^{-iH_{\text{B}}^{(+)}(t-\tau)} \{\rho_{\uparrow\uparrow}(\tau) - \rho_{\downarrow\downarrow}(\tau)\}$$
$$\times e^{iH_{\text{B}}^{(-)}(t-\tau)} + e^{-\xi_+ t} e^{-iH_{\text{B}}^{(+)}t}\rho_{\uparrow\downarrow}(0)e^{iH_{\text{B}}^{(-)}t},$$
(A4a)

$$\rho_{\downarrow\uparrow}(t) = i\gamma_{\text{RF}} \int_0^t d\tau\, e^{-\xi_-(t-\tau)} e^{-iH_{\text{B}}^{(-)}(t-\tau)} \{\rho_{\downarrow\downarrow}(\tau) - \rho_{\uparrow\uparrow}(\tau)\}$$
$$\times e^{iH_{\text{B}}^{(+)}(t-\tau)} + e^{-\xi_- t} e^{-iH_{\text{B}}^{(-)}t}\rho_{\downarrow\uparrow}(0)e^{iH_{\text{B}}^{(+)}t},$$
(A4b)

where we have introduced $\xi_\pm = \frac{\tilde{\Gamma}_{\downarrow}^0}{2} \pm i\delta_{\text{ESR}}$ and $H_{\text{B}}^{(\pm)} = H_{\text{B}} \pm F_{\text{B}}$. To obtain a closed system of equations, the phonon bath is assumed to equilibrate corresponding to the given charge state, i.e., the so-called state-dependent Born factorization [87]. The reduced system and the bath degrees of freedom are factorized as $\rho_{\uparrow\uparrow} \simeq \varrho_{\uparrow\uparrow} \otimes \rho_{\text{B}}^{(+)}$ and $\rho_{\downarrow\downarrow} \simeq \varrho_{\downarrow\downarrow} \otimes \rho_{\text{B}}^{(-)}$, where $\rho_{\text{B}}^{(\pm)} = e^{\beta H_{\text{B}}^{(\pm)}}/\text{tr}_{\text{B}}\{e^{\beta H_{\text{B}}^{(\pm)}}\}$ is the state-dependent thermal density matrix of the phonon bath, and $\beta = (k_{\text{B}}T)^{-1}$ is the inverse temperature.

By substitute Eq. (A4) into Eq. (A3), one arrives at

$$\dot{\varrho}_{00}(t) = -\tilde{\Gamma}_{\uparrow}^{0}\varrho_{00}(t) + \tilde{\Gamma}_{\downarrow}^{\chi_{\downarrow}}\varrho_{\downarrow\downarrow}(t), \tag{A5a}$$

$$\dot{\varrho}_{\uparrow\uparrow}(t) = \tilde{\Gamma}_{\uparrow}^{\chi_{\uparrow}}\varrho_{00}(t) - \int_{0}^{t} d\tau[\gamma^{+}(t-\tau)\varrho_{\uparrow\uparrow}(\tau) \\ - \gamma^{-}(t-\tau)\varrho_{\downarrow\downarrow}(\tau)] - \Upsilon_{0}(t), \tag{A5b}$$

$$\dot{\varrho}_{\downarrow\downarrow}(t) = -\tilde{\Gamma}_{\downarrow}^{0}\varrho_{\downarrow\downarrow}(t) + \int_{0}^{t} d\tau[\gamma^{+}(t-\tau)\varrho_{\uparrow\uparrow}(\tau) \\ - \gamma^{-}(t-\tau)\varrho_{\downarrow\downarrow}(\tau)] + \Upsilon_{0}(t), \tag{A5c}$$

where the inhomogeneity $\Upsilon(t) = [0, -\Upsilon_{0}(t), \Upsilon_{0}(t)]^{\mathrm{T}}$ stems from the initial system bath correlation [53,54,88], as shown in Eqs. (A4a) and (A4b). The inhomogeneity is irrelevant for the full counting statistics in the long-time limit, i.e., zero-frequency cumulants. However, it may have essential roles to play for fluctuations at finite frequencies. It is also worthwhile to mention that in deriving the QME in Eq. (A5), no second-order Born-Markov approximation has been made for the bosonic degrees of freedom. It thus implies that this approach is applicable to the case of strong coupling to a heat bath.

Here, $\gamma^{\pm}(t)$ are bath-assisted hopping rates, given by

$$\gamma^{\pm}(t) = \gamma_{\mathrm{RF}}^{2}\{e^{-\xi_{+}t}C^{(\pm)}(t) + \text{c.c.}\}. \tag{A6}$$

The involving bath correlations are defined as

$$C^{(\pm)}(t) = \mathrm{tr}_{\mathrm{B}}\{e^{-iH_{\mathrm{B}}^{(+)}t}\rho_{\mathrm{B}}^{(\pm)}e^{iH_{\mathrm{B}}^{(-)}t}\}, \tag{A7}$$

which can be calculated exactly to all orders in α using the polaron transformation [89–91]. A detailed derivation is deferred to Appendix B. Here, we just quote the final result: $C^{(\pm)}(t) = e^{-Q(\mp t)}$ with

$$Q(t) = \int_{0}^{\infty} d\omega \frac{J(\omega)}{\omega^{2}}\left\{[1 - \cos(\omega t)]\coth\left(\frac{\beta\omega}{2}\right) + i\sin(\omega t)\right\}. \tag{A8}$$

By switching to Laplace space $\tilde{\varrho}(z) = \int_{0}^{\infty} dt e^{-zt}\varrho(t)$ and similarly for $\tilde{\Upsilon}(z)$, the QME (A5) becomes

$$z\tilde{\varrho}(z) - \varrho(t=0) = \mathcal{W}(\{\chi_{j\sigma}\}, z)\tilde{\varrho}(z) + \tilde{\Upsilon}(z), \tag{A9}$$

where the inhomogeneity is $\tilde{\Upsilon} = [0, -\tilde{\Upsilon}_{0}(z), \tilde{\Upsilon}_{0}(z)]^{\mathrm{T}}$ and the kernel $\mathcal{W}$ reads

$$\mathcal{W}(\{\chi_{j\sigma}\}, z) = \begin{pmatrix} -\tilde{\Gamma}_{\uparrow}^{0} & 0 & \tilde{\Gamma}_{\downarrow}^{\chi_{\downarrow}} \\ \tilde{\Gamma}_{\uparrow}^{\chi_{\uparrow}} & -\gamma_{z}^{+} & \gamma_{z}^{-} \\ 0 & \gamma_{z}^{+} & -\gamma_{z}^{-} - \tilde{\Gamma}_{\downarrow}^{0} \end{pmatrix}. \tag{A10}$$

Here the bath-assisted hopping rates $\gamma_{z}^{\pm}$ are obtained by Laplace transform of Eq. (A6)

$$\gamma_{z}^{\pm} = \gamma_{\mathrm{RF}}^{2}\{\tilde{C}^{(\pm)}(z_{+}) + \tilde{C}^{(\mp)}(z_{-})\}, \tag{A11}$$

with $z_{\pm} = z + \frac{\tilde{\Gamma}_{\downarrow}^{0}}{2} \pm i\delta_{\mathrm{ESR}}$ and $\tilde{C}^{(\pm)}(z)$ the Laplace transform of the bath correlation function. We assume the spin system evolves from $t = -\infty$ and the reduced system reached

the steady state $\varrho(\{N_{j\sigma}\}, t) = \delta_{\{N_{j\sigma}\}, \{0\}}\varrho^{\mathrm{st}}$ at $t = 0$. For this model the inhomogeneity is independent of the spin-resolved counting fields [53]:

$$\tilde{\Upsilon}(z) = \frac{\mathcal{W}_{0} - \mathcal{W}(\{\chi_{j\sigma}\} = \{0\}, z)}{z}\varrho^{\mathrm{st}}, \tag{A12}$$

where $\varrho^{\mathrm{st}} = |0\rangle\rangle$ is the steady state obtained as the normalized solution to $\mathcal{W}_{0}|0\rangle\rangle = 0$.

APPENDIX B: DERIVATION OF THE BATH CORRELATION FUNCTIONS

We consider the polaron transformation

$$U^{(\pm)} = e^{\pm iS}, \quad S = \sum_{q}\frac{i\lambda_{q}}{\omega_{q}}(a_{q} - a_{q}^{\dagger}), \tag{B1}$$

which will removes F_{B} from the bath correlation functions. By using the Baker-Campbell-Hausdorff (BCH) relation

$$e^{X}Ye^{-X} = \sum_{0}^{\infty}\frac{1}{n!}[X, Y]_{n}, \tag{B2}$$

with $[X, Y]_{n+1} = [X, [X, Y]_{n}]$ and $[X, Y]_{0} = Y$, the bosonic annihilation and creation operators are transformed to

$$U^{(\pm)}a_{q}[U^{(\pm)}]^{\dagger} = a_{q} \mp \frac{\lambda_{q}}{\omega_{q}}, \tag{B3a}$$

$$U^{(\pm)}a_{q}^{\dagger}[U^{(\pm)}]^{\dagger} = a_{q}^{\dagger} \mp \frac{\lambda_{q}}{\omega_{q}}. \tag{B3b}$$

Straightforwardly, the effective bath Hamiltonians $H_{\mathrm{B}}^{(\pm)} = H_{\mathrm{B}} \pm F_{\mathrm{B}}$ under the transformation are given by

$$U^{(\pm)}H_{\mathrm{B}}^{(\pm)}[U^{(\pm)}]^{\dagger} = H_{\mathrm{B}} - \sum_{q}\frac{\lambda_{q}^{2}}{2\omega_{q}}, \tag{B4}$$

which leads directly to

$$U^{(\pm)}e^{\pm iH_{\mathrm{B}}^{(\pm)}t}[U^{(\pm)}]^{\dagger} = e^{\pm i(H_{\mathrm{B}} - \sum_{q}\frac{\lambda_{q}^{2}}{2\omega_{q}})t}, \tag{B5}$$

$$U^{(\pm)}e^{-\beta H_{\mathrm{B}}^{(\pm)}}[U^{(\pm)}]^{\dagger} = e^{-\beta(H_{\mathrm{B}} - \sum_{q}\frac{\lambda_{q}^{2}}{2\omega_{q}})}. \tag{B6}$$

By insertion of the identity $1^{(\pm)} = U^{(\pm)}[U^{(\pm)}]^{\dagger}$ in the bath correlation functions in Eq. (A7), one arrives at

$$C^{(\pm)}(t) = \mathrm{tr}_{\mathrm{B}}\{1^{(+)}e^{-iH_{\mathrm{B}}^{(+)}t}1^{(+)}1^{(\pm)}\rho_{\mathrm{B}}^{(\pm)}1^{(\pm)}1^{(-)}e^{iH_{\mathrm{B}}^{(-)}t}1^{(-)}\} \\ = \langle e^{\pm iS(0)}e^{\mp iS(\pm t)}\rangle_{\mathrm{B}}, \tag{B7}$$

where $S(t) = e^{iH_{\mathrm{B}}t}Se^{-iH_{\mathrm{B}}t} = \sum_{q}\frac{i\lambda_{q}}{\omega_{q}}(a_{q}e^{-i\omega_{q}t} - a_{q}^{\dagger}e^{i\omega_{q}t})$ and $\langle\cdots\rangle_{\mathrm{B}} = \mathrm{tr}_{\mathrm{B}}\{(\cdots)\rho_{\mathrm{B}}\}$ stands for the average over degrees of freedom of the boson bath, with $\rho_{\mathrm{B}} = e^{-\beta H_{\mathrm{B}}}/\mathrm{tr}_{\mathrm{B}}\{e^{-\beta H_{\mathrm{B}}}\}$ the local thermal equilibrium state of boson bath.

By recalling the BCH relation $e^X e^Y = e^{X+Y} e^{\frac{1}{2}[X,Y]}$, Eq. (B7) can be rewritten as

$$C^{(\pm)} = \langle e^{\pm iS(0) \mp iS(\pm t)} e^{\frac{1}{2}[S(0),S(\pm t)]} \rangle_B, \qquad (B8)$$

where

$$\frac{1}{2}[S(0),S(\pm t)] = \pm i \sum_q \frac{\lambda_q^2}{\omega_q^2} \sin(\omega_q t) \qquad (B9)$$

is just a c-number, and

$$e^{\pm iS(0) \mp iS(\pm t)} = \exp\left\{ \pm \sum_q \frac{\lambda_q}{\omega_q}[a_q^\dagger(1 - e^{\pm i\omega_q t}) - \text{H.c.}]\right\}. \qquad (B10)$$

For a thermal state $\rho_B \propto e^{-\beta H_B}$, it is easy to verify that for an arbitrary complex c-number z_q one has the following relation [91]

$$\left\langle e^{\pm \sum_q \{z_q^* a_q^\dagger - \text{h.c.}\}} \right\rangle_B = e^{-\sum_q |z_q|^2 [n_B(\omega_q) + 1/2]}, \qquad (B11)$$

where $n_B(\omega_q) = \{e^{\beta\omega_q} - 1\}^{-1}$ is the Bose distribution. By substituting Eqs. (B9) and (B11) into Eq. (B8), one eventually

arrives at the bath correlations

$$C^{(\pm)}(t) = e^{-Q(\mp t)}$$

$$Q(t) = \int_0^\infty d\omega \frac{J(\omega)}{\omega^2} \left\{ [1 - \cos(\omega t)] \coth\left(\frac{\beta\omega}{2}\right) + i\sin(\omega t)\right\}, \qquad (B12)$$

where $J(\omega) = \sum_q |\lambda_q|^2 \delta(\omega - \omega_q)$ is the spectral function of the heat bath.

Specifically, for Ohmic spectral $J(\omega) = 2\alpha\omega e^{-\omega/\omega_c}$ and at zero temperature $(1/\beta = k_B T = 0)$, the bath correlation functions are reduced to

$$C^{(\pm)}(t) = (1 \pm i\omega_c t)^{-2\alpha}. \qquad (B13)$$

Their counterparts in the Laplace domain are then given by

$$\tilde{C}^{(\pm)}(z) = (\pm i\omega_c)^{-2\alpha} z^{2\alpha-1} e^{\mp \frac{iz}{\omega_c}} \Gamma\left(1 - 2\alpha, \mp\frac{iz}{\omega_c}\right), \qquad (B14)$$

where $\Gamma(\cdots, \cdots)$ stands for the incomplete Γ function.

---

[1] Y. M. Blanter and M. Büttiker, Phys. Rep. **336**, 1 (2000).

[2] T. Fujisawa, T. Hayashi, R. Tomita, and Y. Hirayama, Science **312**, 1634 (2006).

[3] S. Gustavsson, R. Leturcq, B. Simovic, R. Schleser, T. Ihn, P. Studerus, K. Ensslin, D. C. Driscoll, and A. C. Gossard, Phys. Rev. Lett. **96**, 076605 (2006).

[4] S. Gustavsson, R. Leturcq, M. Studer, I. Shorubalko, T. Ihn, K. Ensslin, D. Driscoll, and A. Gossard, Surf. Sci. Rep. **64**, 191 (2009).

[5] S. Gustavsson, R. Leturcq, M. Studer, T. Ihn, K. Ensslin, D. C. Driscoll, and A. C. Gossard, Nano Lett. **8**, 2547 (2008).

[6] E. V. Sukhorukov, A. N. Jordan, S. Gustavsson, R. Leturcq, T. Ihn, and K. Ensslin, Nat. Phys. **3**, 243 (2007).

[7] J. M. Elzerman, R. Hanson, L. H. W. van Beveren, B. Witkamp, L. M. K. Vandersypen, and L. P. Kouwenhoven, Nature (London) **430**, 431 (2004).

[8] M. Xiao, I. Martin, E. Yablonovitch, and H. Jiang, Nature (London) **430**, 435 (2004).

[9] S. Amasha, K. MacLean, I. P. Radu, D. M. Zumbühl, M. A. Kastner, M. P. Hanson, and A. C. Gossard, Phys. Rev. B **78**, 041306 (2008).

[10] R. Hanson, L. H. Willems van Beveren, I. T. Vink, J. M. Elzerman, W. J. M. Naber, F. H. L. Koppens, L. P. Kouwenhoven, and L. M. K. Vandersypen, Phys. Rev. Lett. **94**, 196802 (2005).

[11] A. Morello, J. J. Pla, F. A. Zwanenburg, K. W. Chan, K. Y. Tan, H. Huebl, M. Möttönen, C. D. Nugroho, C. Yang, J. A. van Donkelaar *et al.*, Nature (London) **467**, 687 (2010).

[12] D. A. Bagrets and Y. V. Nazarov, Phys. Rev. B **67**, 085316 (2003).

[13] Y. V. Nazarov, *Quantum Noise in Mesoscopic Physics* (Kluwer Academic Publishers, Dordrecht, 2003).

[14] Y. M. Blanter, in *Recent Advances in Studies of Current Noise* (Springer, Berlin, 2011), pp. 55–74.

[15] J. Wei and V. Chandrasekhar, Nat. Phys. **6**, 494 (2010).

[16] R. Mélin, C. Benjamin, and T. Martin, Phys. Rev. B **77**, 094512 (2008).

[17] D. Chevallier, J. Rech, T. Jonckheere, and T. Martin, Phys. Rev. B **83**, 125421 (2011).

[18] J. Nilsson, A. R. Akhmerov, and C. W. J. Beenakker, Phys. Rev. Lett. **101**, 120403 (2008).

[19] K. T. Law, P. A. Lee, and T. K. Ng, Phys. Rev. Lett. **103**, 237001 (2009).

[20] G. Strübi, W. Belzig, M.-S. Choi, and C. Bruder, Phys. Rev. Lett. **107**, 136403 (2011).

[21] P. Wang, Y. Cao, M. Gong, G. Xiong, and X.-Q. Li, Europhys. Lett. **103**, 57016 (2013).

[22] H.-F. Lü, H.-Z. Lu, and S.-Q. Shen, Phys. Rev. B **90**, 195404 (2014).

[23] A. N. Jordan and M. Büttiker, Phys. Rev. Lett. **95**, 220401 (2005).

[24] H. J. Jiao, F. Li, S.-K. Wang, and X.-Q. Li, Phys. Rev. B **79**, 075320 (2009).

[25] I. Chernii and E. V. Sukhorukov, Phys. Rev. B **85**, 205438 (2012).

[26] J. Y. Luo, H. J. Jiao, J. Hu, X.-L. He, X. L. Lang, and S.-K. Wang, Phys. Rev. B **92**, 045107 (2015).

[27] Z. Tan, T. Nieminen, A. Puska, J. Sarkar, P. Lähteenmäki, F. Duerr, C. Gould, L. Molenkamp, K. Nagaev, and P. Hakonen, arXiv:1602.00290.

[28] M. Büttiker, Phys. Rev. Lett. **65**, 2901 (1990).

[29] M. Büttiker, Phys. Rev. B **46**, 12485 (1992).

[30] M. Henny, S. Oberholzer, C. Strunk, T. Heinzel, K. Ensslin, M. Holland, and C. Schönenberger, Science **284**, 296 (1999).

[31] W. D. Oliver, J. Kim, R. C. Liu, and Y. Yamamoto, Science **284**, 299 (1999).

[32] D. Urban and J. König, Phys. Rev. B **79**, 165319 (2009).

[33] H.-F. Lu, J.-R. Zhang, T. Wu, X.-T. Zu, and H.-W. Zhang, J. Appl. Phys. **107**, 034314 (2010).

[34] J. Y. Luo, H. J. Jiao, Y. Shen, G. Cen, X.-L. He, and C. Wang, J. Phys.: Condens. Matter **23**, 145301 (2011).

[35] R.-Q. Wang, L. Sheng, L.-B. Hu, B. G. Wang, and D. Y. Xing, Phys. Rev. B **84**, 115304 (2011).

[36] B. H. Wu and J. C. Cao, Phys. Rev. B **81**, 125326 (2010).

[37] J. Y. Luo, J. Hu, X. L. Lang, Y. Shen, X.-L. He, and H. J. Jiao, Phys. Lett. A **378**, 892 (2014).

[38] N. Ubbelohde, C. Fricke, F. Hohls, and R. J. Haug, Phys. Rev. B **88**, 041304 (2013).

[39] M. Misiorny, I. Weymann, and J. Barnaś, Phys. Rev. B **79**, 224420 (2009).

[40] I. Weymann, B. R. Bułka, and J. Barnaś, Phys. Rev. B **83**, 195302 (2011).

[41] Y. Okazaki, S. Sasaki, and K. Muraki, Phys. Rev. B **87**, 041302 (2013).

[42] M. Flöser, D. Feinberg, and R. Mélin, Phys. Rev. B **88**, 094517 (2013).

[43] J. Börlin, W. Belzig, and C. Bruder, Phys. Rev. Lett. **88**, 197001 (2002).

[44] P. Samuelsson and M. Büttiker, Phys. Rev. Lett. **89**, 046601 (2002).

[45] S.-T. Wu and S. Yip, Phys. Rev. B **72**, 153101 (2005).

[46] Y. Chen and R. A. Webb, Phys. Rev. Lett. **97**, 066604 (2006).

[47] S. Oberholzer, E. Bieri, C. Schonenberger, M. Giovannini, and J. Faist, Phys. Rev. Lett. **96**, 046804 (2006).

[48] D. T. McClure, L. DiCarlo, Y. Zhang, H.-A. Engel, C. M. Marcus, M. P. Hanson, and A. C. Gossard, Phys. Rev. Lett. **98**, 056801 (2007).

[49] A. Das, Y. Ronen, M. Heiblum, D. Mahalu, A. V. Kretinin, and H. Shtrikman, Nat. Commun. **3**, 1165 (2012).

[50] Y. Zhang, L. DiCarlo, D. T. McClure, M. Yamamoto, S. Tarucha, C. M. Marcus, M. P. Hanson, and A. C. Gossard, Phys. Rev. Lett. **99**, 036603 (2007).

[51] A. Cottet, W. Belzig, and C. Bruder, Phys. Rev. Lett. **92**, 206801 (2004).

[52] A. Cottet, W. Belzig, and C. Bruder, Phys. Rev. B **70**, 115315 (2004).

[53] C. Flindt, T. Novotný, A. Braggio, M. Sassetti, and A.-P. Jauho, Phys. Rev. Lett. **100**, 150601 (2008).

[54] C. Flindt, T. Novotný, A. Braggio, and A.-P. Jauho, Phys. Rev. B **82**, 155407 (2010).

[55] S. A. Gurvitz and Y. S. Prager, Phys. Rev. B **53**, 15932 (1996).

[56] X. Q. Li, J. Y. Luo, Y. G. Yang, P. Cui, and Y. J. Yan, Phys. Rev. B **71**, 205304 (2005).

[57] J. Y. Luo, J. Jin, S.-K. Wang, J. Hu, Y. Huang, and X.-L. He, Phys. Rev. B **93**, 125122 (2016).

[58] R. Zwanzig, *Nonequilibrium Statistical Mechanics* (Oxford University Press, New York, 2001).

[59] A. Braggio, J. König, and R. Fazio, Phys. Rev. Lett. **96**, 026805 (2006).

[60] Y. Makhlin, G. Schön, and A. Shnirman, Rev. Mod. Phys. **73**, 357 (2001).

[61] J. König, H. Schoeller, and G. Schön, Phys. Rev. Lett. **76**, 1715 (1996).

[62] O. Sauret and D. Feinberg, Phys. Rev. Lett. **92**, 106601 (2004).

[63] J. Y. Luo, H. J. Jiao, B. T. Xiong, X.-L. He, and C. Wang, J. Phys.: Condens. Matter **25**, 155304 (2013).

[64] M.-S. Choi, F. Plastina, and R. Fazio, Phys. Rev. Lett. **87**, 116601 (2001).

[65] Y. Ronena, Y. Cohena, J.-H. Kanga, A. Haima, M.-T. Riedera, M. Heibluma, D. Mahalua, and H. Shtrikmana, Proc. Natl. Acad. Sci. USA **113**, 1743 (2015).

[66] R. de Picciotto, M. Reznikov, M. Heiblum, V. Umansky, G. Bunin, and D. Mahalu, Nature **389**, 162 (1997).

[67] M. Hashisaka, T. Ota, K. Muraki, and T. Fujisawa, Phys. Rev. Lett. **114**, 056802 (2015).

[68] M. Dolev, Y. Gross, Y. C. Chung, M. Heiblum, V. Umansky, and D. Mahalu, Phys. Rev. B **81**, 161303 (2010).

[69] E.-A. Kim, M. J. Lawler, S. Vishveshwara, and E. Fradkin, Phys. Rev. B **74**, 155324 (2006).

[70] B. Elattari and S. A. Gurvitz, Phys. Lett. A **292**, 289 (2002).

[71] S. A. Tarasenko, V. I. Perel', and I. N. Yassievich, Phys. Rev. Lett. **93**, 056601 (2004).

[72] M. M. Glazov, P. S. Alekseev, M. A. Odnoblyudov, V. M. Chistyakov, S. A. Tarasenko, and I. N. Yassievich, Phys. Rev. B **71**, 155313 (2005).

[73] I. V. Rozhansky and N. S. Averkiev, Phys. Rev. B **77**, 115309 (2008).

[74] J. Silvano de Sousa and J. Smoliner, Phys. Rev. B **85**, 085303 (2012).

[75] P. Stano and P. Jacquod, Phys. Rev. B **82**, 125309 (2010).

[76] T.-M. Chen, A. C. Graham, M. Pepper, F. Sfigakis, I. Farrer, and D. A. Ritchie, Phys. Rev. B **79**, 081301 (2009).

[77] M. Julliere, Phys. Lett. A **54**, 225 (1975).

[78] G. Kießlich, E. Schöll, T. Brandes, F. Hohls, and R. J. Haug, Phys. Rev. Lett. **99**, 206602 (2007).

[79] R. Sánchez, G. Platero, and T. Brandes, Phys. Rev. Lett. **98**, 146805 (2007).

[80] A. Thielmann, M. H. Hettler, J. König, and G. Schön, Phys. Rev. B **71**, 045341 (2005).

[81] J. Y. Luo, S.-K. Wang, X.-L. He, X.-Q. Li, and Y. J. Yan, J. Appl. Phys. **108**, 083720 (2010).

[82] H. M. Wiseman and G. J. Milburn, *Quantum Measurement and Control* (Cambridge University Press, Cambridge, 2010).

[83] N. Ubbelohde, C. Fricke, C. Flindt, F. Hohls, and R. J. Haug, Nat. Commun. **3**, 612 (2012).

[84] M. Creux, A. Crépieux, and T. Martin, Phys. Rev. B **74**, 115323 (2006).

[85] D. K. C. MacDonald, *Noise and Fluctuations: An Introduction* (Wiley, New York, 1962), Chap. 2.2.1.

[86] R. Aguado and T. Brandes, Phys. Rev. Lett. **92**, 206601 (2004).

[87] C. Flindt, T. Novotný, and A.-P. Jauho, Phys. Rev. B **70**, 205334 (2004).

[88] J. Y. Luo, H. J. Jiao, B. T. Xiong, X.-L. He, and C. R. Wang, J. Appl. Phys. **114**, 173703 (2013).

[89] T. Brandes, Phys. Rep. **408**, 315 (2005).

[90] U. Weiss, *Quantum Dissipative Systems*, 3rd ed. (World Scientific, Singapore, 2008).

[91] T. Krause, T. Brandes, M. Esposito, and G. Schaller, J. Chem. Phys. **142**, 134106 (2015).